iodine-123-BMIPP myocardial imaging for myocardial infarction and hypertrophic cardiomyopathy. *Ann Nucl Med* 1993;7:35–40.
21. Kurata C, Tawahara K, Okayama K, Wakabayashi Y, Kobayashi A, Yamazaki N, Kaneko M. Myocardial imaging with radioiodinated beta-methyl-branched fatty acid in cardiomyopathy. *Ann Nucl Med* 1993;7:27–34.
22. Morita K, Yanagimoto S, Otsuka N, et al. Iodine-123-BMIPP scintigraphy in seven cases with cardiomyopathy. *Ann Nucl Med* 1993;7:101–107.
23. Buchanan MV, Hettich RL. Fourier transform mass spectrometry of high-mass biomolecules. *Anal Chem* 1993;65:245A–259A.
24. Knapp FF Jr, Goodman MM, Callahan AP, Kirsch G. Radioiodinated 15-(p-iodophenyl)-3,3-dimethylpentadecanoic acid: a useful new agent to evaluate myocardial fatty acid uptake. *J Nucl Med* 1986;27:521–531.
25. Stremmel W. Fatty acid uptake by isolated rat heart myocytes represents a carrier-mediated transport process. *J Clin Invest* 1988;81:844–852.
26. Glatz JFC, van der Vusse GJ, Reneman RS. Protective role of fatty acid-binding protein in ischemic and reperfused heart. *Circ Res* 1991;68:1490–1491.
27. Lam LKP, Hui RAHF, Jones JB. Enzymes in organic synthesis: stereoselective pig liver esterase catalyzed hydrolyses of 3-substituted glutarate diesters; optimization of enantiomeric excess through a reaction conditions control. *J Org Chem* 1986;51:2047–2050.
28. Konoike T, Araki Y. Practical synthesis of chiral synthons for the preparation of HMG-CoA reductase inhibitors. *J Org Chem* 1994;59:7849–7854.
29. Kiratake J, Inagaki M, Yamamoto Y, Oda J. Enaniotropic-group differentiation: catalytic asymmetric ring-opening of prochiral cyclic acid anhydrides with methanol, using chinchona alkaloids. *J Chem Soc Perkin Trans* 1987:1053–1058.
30. Ambrose KR, Owen BA, Goodman MM, Knapp FF Jr. Evaluation of the metabolism in rat hearts of two new radioiodinated 3-methyl-branched fatty acid myocardial imaging agents. *Eur J Nucl Med* 1987;2:486–491.
31. Ambrose KR, Owen BA, Callahan AP, Goodman MM, Knapp FF Jr. Effects of fasting on the myocardial subcellular distribution and lipid distribution of terminal p-iodophenyl-substituted fatty acids in rats. *Nucl Med Biol* 1988;15:695–700.
32. Knapp FF Jr, Goodman MM, Reske SN, et al. Radioiodinated methyl-branched fatty acids: evaluation of catabolites formed in vivo. *NucCompact/Eur Am Commun Nucl Med* 1990;21:229–231.
33. Kropp J, Ambrose KR, Knapp FF Jr, Nissen HP, Biersack H-J. Incorporation of IPPA and BMIPP fatty acid analogs into complex lipids from isolated rat hearts. *Nucl Med Biol* 1992;19:283–288.
34. Morishita S, Kusuoka H, Yamamichi Y, Suzuki N, Kurami M, Nishimura T. Kinetics of radioiodinated species in subcellular fractions from rat hearts following administration of iodine-123-labeled 15-(p-iodophenyl)-3-(R,S)-methylpentadecanoic acid (^{123}I-BMIPP). *Eur J Nucl Med* 1996;23:383–389.
35. Yamamichi Y, Kusuoka H, Morishita K, et al. Metabolism of iodine-123-labeled 15-(p-iodophenyl)-3-(R,S)-methylpentadecanoic acid (BMIPP) in perfused rat hearts. *J Nucl Med* 1995;36:1043–1050.

Clinical Validation of Automatic Quantitative Defect Size in Rest Technetium-99m-Sestamibi Myocardial Perfusion SPECT

Xingping Kang, Daniel S. Berman, Kenneth F. Van Train, Aman M. Amanullah, Joseph Areeda, John D. Friedman, Hosen Kiat and Guido Germano

Division of Nuclear Medicine, Department of Imaging; Division of Cardiology, Department of Medicine, Cedars-Sinai Medical Center, The CSMC Burns & Allen Research Institute, and Department of Medicine, University of California Los Angeles, School of Medicine, Los Angeles, California

We examined the relationships of automatic quantitative perfusion defect size and defect severity to rest left ventricular ejection fraction and semiquantitative visual sestamibi defect size in rest ^{99m}Tc-sestamibi SPECT in 40 consecutive patients with a history of myocardial infarction more than 30 days prior to testing. The purpose of this investigation was to validate the use of automatic quantitative rest sestamibi SPECT as a clinical measure of assessing relative infarction size. **Methods:** All patients received 20–30 mCi of ^{99m}Tc-sestamibi followed by SPECT imaging. Quantitative defect analysis used previously developed resting normal limits and an automatic version of a commercially available quantitative program (CEqual). Semiquantitative visual defect interpretation used a 20 segment/scan and five-point scoring analysis. First-pass (FP) radionuclide ventriculography (RVG) and gated sestamibi perfusion SPECT were each performed in 31 patients. **Results:** LVEF assessed by FP RVG was 37% ± 15% (range 14%–62%) and 37% ± 16% (range 12%–63%) by gated perfusion SPECT with high linear correlation ($r = 0.96$, $n = 22$) between the two methods. Myocardial perfusion defect size was 24% ± 15% of LV (range 0%–50%) and defect severity was 1103 ± 864 (range 0 to 2825) by automatic quantitative rest sestamibi. Perfusion defect size and defect severity both had close correlations with LVEF by FP RVG ($r = -0.78$, $r = -0.86$) and by gated perfusion SPECT ($r = -0.75$, $r = -0.79$). High linear correlations were observed between quantitative defect size and summed visual score of segments with score ≥2 ($r = 0.82$) and the number of visually abnormal segments ($r = 0.77$), as well as between defect severity and visual summed rest score ($r = 0.86$) and the number of visually abnormal segments ($r = 0.76$). **Conclusion:** Quantitation of rest sestamibi SPECT defect extent and severity using automatic CEqual correlates well with rest LVEF and with semiquantitative expert visual analysis. Results of this study define a strong relationship between measurements of ^{99m}Tc-sestamibi perfusion defect as measured by an automatic software program and global left ventricular function. The automatic quantitative program appears to be a useful measure of assessing infarct size in patients with remote myocardial infarction.

Key Words. technetium-99m-sestamibi; myocardial perfusion; myocardial infarction; left ventricular function; SPECT

J Nucl Med 1997; 38:1441–1446

The extent of left ventricular (LV) perfusion defect on rest ^{99m}Tc-sestamibi SPECT has been shown to reflect the size of myocardial infarction (*1–3*). The size of myocardial infarction has been shown to be a strong predictor of long-term survival (*4*). Therefore, a readily available, accurate method for the noninvasive measurement of infarct size could provide important prognostic information. In clinical practice, assessment of perfusion defect size is most widely performed with subjective visual analysis (*5*). We have previously developed normal limits and criteria of abnormality for quantitative analysis of rest sestamibi perfusion SPECT, resulting in an automatic quantitative approach which could provide an objective reproducible way to assess perfusion defect size. Since left ventricular ejection fraction (LVEF) has been shown to be inversely proportional to infarction size (*6,7*), we sought to validate the automatic quantitative defect size in rest sestamibi myocardial perfusion SPECT as a clinical measure of assessing infarct size

Received Sept. 23, 1996; revision accepted Dec. 19, 1996.

For correspondence or reprints contact: Daniel S. Berman, MD, Department of Imaging, Cedars-Sinai Medical Center, 8700 Beverly Blvd; Rm. A042, Los Angeles, CA 90048.

by comparing it with rest LVEF and with semiquantitative visual defect size in patients with prior myocardial infarction.

METHODS

Patients

The study group consisted of 40 consecutive patients with a history of documented myocardial infarction more than 30 days (25 patients more than 6 mos) prior to testing who were referred for rest sestamibi SPECT imaging. There were 31 men and 9 women with a mean age of 67 yr (range 40–87 yr). Patients with cardiomyopathy, valvular heart disease or atrial fibrillation were excluded, the latter because of potential inaccuracy of measurement of LVEF, as were patients with recent (less than 90 days) coronary artery bypass grafting (CABG) or percutaneous transluminal coronary angioplasty (PTCA). History of remote prior CABG was present in 17 patients (42.5%) and remote PTCA in 14 patients (35.0%).

Myocardial Perfusion SPECT

Resting sestamibi SPECT was performed with patients supine 1 hr after injection of 20–30 mCi of sestamibi. All SPECT studies utilized a scintillation camera/computer system equipped with a high resolution collimator. Images were acquired over 180° in 3° steps, commencing in the 45° right anterior oblique position and ending in the 45° left posterior oblique position. Image acquisition was performed with a 20% energy window on the 140 keV peak of sestamibi, using 64 × 64 image matrices, as previously described (*5,8*). The raw projection data were automatically reconstructed using a previously developed algorithm (*9,10*) which consists of three software modules. These modules determine the reconstruction limits for the projection data, reconstruct the raw projection data into 6-mm thick transaxial tomograms, and reorient the transaxial data into short-axis, vertical and horizontal long axis tomograms without operator intervention. No attenuation or scatter correction was used.

Computer Quantification of Myocardial Perfusion SPECT

Resting sestamibi tomograms were quantified automatically using a modification of the Cedars-Sinai computerized two-dimensional polar maps software (CEqual). Analysis begins by automatically identifying the left ventricle using the algorithm described by Germano et al. (*11*). This identification is based on a clustering algorithm applied to short axis reconstructed tomograms. By applying adaptive thresholding to iteratively define clusters corresponding to expected ventricular volumes, the algorithm separates myocardium from potential extracardiac structures reflecting hepatic, splenic or gut activity. If the results of the clustering approach fails to meet certain criteria the algorithm is enhanced by application of a Hough transform and a scoring function weighted to favor a doughnut-like configuration. The remaining portions of the algorithm are those originally described by Garcia (*12*). The left ventricle is described by an apex and base location, with a center coordinate and average radius. Maximal count circumferential profiles are generated using a spherical search for the apex and a cylindrical search of the remaining LV. The pixel locations corresponding to the maximal myocardial counts, as well as the count values, are used to improve the descriptive values. The LV radius is reset to the average radius in the circumferential profiles, and the basal slice is limited to the slice with a maximum count of 50% or less than that of the hottest myocardial slice. The final sampling of the myocardium is made using these values. Myocardial sampling consists of generation of maximum count circumferential profiles using a spherical search for the apical and a cylindrical search for the remainder of the short-axis tomograms. The rest profiles are normalized to the most normal wall of the patient's entire rest study prior to comparison to the resting normal limits (*13*). These high dose resting normal limits were derived from a 20-mCi ^{99m}Tc-sestamibi injection as part of a two-day, rest-stress protocol (*14*). A quality control report is generated to allow operator verification of the performance of the automatic algorithm, or to manually correct any sub-optimal values. Then the values are plotted in a two-dimensional polar map representing the entire left ventricular myocardium. The criteria for abnormality used for this evaluation were determined by receiver operating characteristic (ROC) curve analysis of the regional standard deviations from the mean that best separated visually normal from abnormal resting myocardial perfusion. These optimal standard deviations were used as thresholds of abnormality for the total and three major regions (LAD, LCX and RCA) of the myocardium. Quantitative defect extent was defined by summation of the number of profile points falling below the normal limit expressed as percentage of perfusion defect, and quantitative defect "severity" (actually a measure of defect extent and severity) was defined by the sum of the product of all profile points below the normal limits multiplied by their respective standard deviation below the normal mean count (Fig. 1). The defect extent is initially determined then the severity is calculated by examining the pixels confined to the area defined by the defect extent.

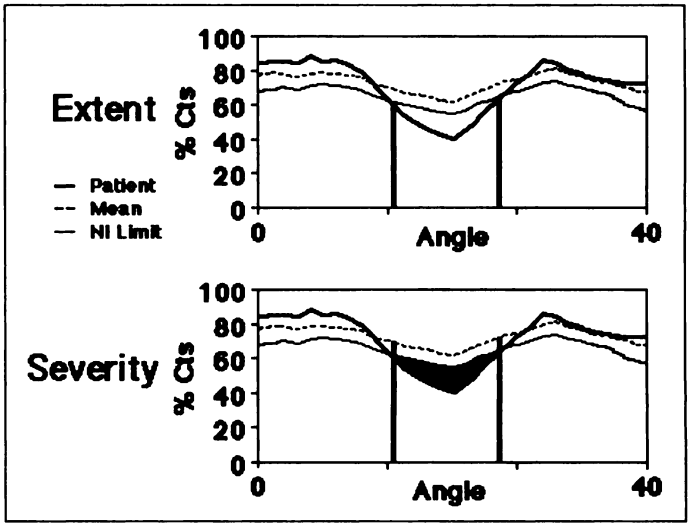

FIGURE 1. Defect extent represents the number of pixels which fell below the normal limit (% abnormal) and defect severity represents the degree of abnormality within the defined defect zone measured by the area between the patients profile and the normal limit profile.

Visual Analysis of Myocardial Perfusion SPECT

Visual interpretation of SPECT perfusion images used short-axis and vertical long-axis tomograms divided into 20 segments for each patient (*5*). These segments were assigned to six evenly spaced regions in apical, midventricular and basal slices of the short-axis views and two apical segments on the midventricular long-axis slice. Segments were scored by an expert using a five-point scoring system (0 = normal; 1 = equivocal; 2 = moderate; 3 = severe reduction of radioisotope uptake; 4 = absence of detectable radiotracer in the segment). Apparent perfusion defects which were considered to be caused by soft tissue attenuation were assigned a score of 1. The observer was unaware of the patient's clinical history. Segments with score of ≥2 were defined as abnormal segments. The summed rest score was then obtained by adding the rest scores of the abnormal segments. The summed rest score and the number of abnormal segments were compared to the quantitative sestamibi defect measurements.

First-pass Radionuclide Ventriculography (RVG)

A rest first-pass RVG was recorded using a bolus injection of 20–30 mCi sestamibi. As the bolus passed through the heart and lungs, images were acquired in the anterior projection using a multicrystal gamma camera. Forty scintigraphic frames per second for a total of 25 sec were obtained using a high-sensitivity collimator and an 18% window centered over the 140-keV photopeak of ^{99m}Tc. The RVGs were processed with a commercial software package. Briefly, the algorithms sequentially perform the following: dead time and uniformity correction, temporal smoothing, creation of a preliminary LV representative cycle, background modification, and creation of a final representative cycle (*15,16*). LVEF was calculated from the counts change of the background-corrected representative cycle using a dual region of interest algorithm.

Gated Sestamibi Perfusion SPECT

Sestamibi gated perfusion SPECT images were acquired on a triple-detector camera (Prism 3000, Picker, OH) with 25 sec of data collection per projection, distributed over eight frames per cardiac cycle, and no arrhythmia rejection. The cardiac beat length acceptance window was set at 100%. LVEF was calculated by using a completely automatic algorithm which operates in the three-dimensional space. It segments the LV, estimates and displays endocardial and epicardial surfaces for all gating intervals in the cardiac cycle, calculates the relative LV cavity volumes, and derives the global EF from the end-diastolic and end systolic volume (*11*). For perfusion defect amount the gated data were summed to form an ungated SPECT dataset.

Statistical Analysis

Data are expressed as means ±1 s.d. Simple linear regression analysis was used to correlate quantitative rest sestamibi perfusion defects and severity to LVEF, visual summed rest score, number of abnormal segments and correlate LVEF from FP to LVEF from gated perfusion SPECT. Comparison of the relationships between quantitative defect size and LVEF in the anterior MI and inferior MI groups was evaluated by analysis of covariance. A value of $p < 0.05$ was considered statistically significant.

RESULTS

LVEF from First-pass RVG and Gated Perfusion SPECT

Mean LVEF assessed from FP RVG in 31 patients was 37% ± 15% (range 14%–62%) and from gated perfusion SPECT in 31 patients was 37% ± 16% (range 12%–63%). Twenty-two patients underwent both FP RVG and gated perfusion SPECT. There was a high correlation between LVEF assessed by these two methods ($r = 0.96$, s.e.e. = 3.61, $p < 0.001$).

Relationship between Quantitative Sestamibi Defect and LVEF

Myocardial perfusion defect size by automatic quantitative rest sestamibi was 24% ± 15% of LV (range 0%–50%) and defect severity was 1103 ± 864 (range 0%–2825). Quantitative defect size correlated closely with LVEF from FP RVG and from gated SPECT ($r = -0.78$ and $r = -0.75$, $n = 31$, Fig. 2). Quantitative defect severity correlated even better with LVEF from FP and from gated SPECT ($r = -0.86$ and $r = -0.79$, $n = 31$, Fig. 3).

Correlations of Anterior and Inferior Wall Perfusion Defects with LVEF

The location of a perfusion defect was in the anterior wall in 15 patients and in the inferior wall in 22 patients. Correlation between quantitative rest sestamibi defect size and LVEF tended to be higher in patients with anterior wall defects than in those with inferior wall defects in both FP and gated SPECT groups ($r = -0.94$ and $r = -0.77$ versus $r = -0.71$ and $r = -0.61$, respectively). However, probably due to the small numbers of patients in each group, the differences of the two regression relationships by analysis of covariance were not statistically significant ($p > 0.05$).

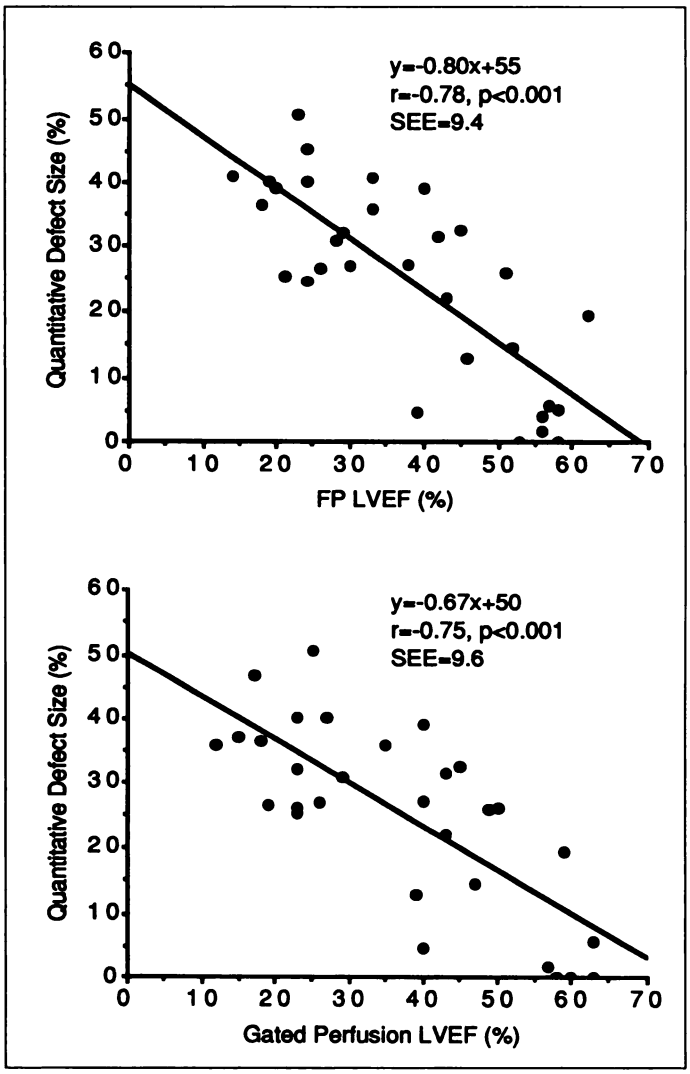

FIGURE 2. Correlation between quantitative rest ^{99m}Tc-sestamibi perfusion defect size and LVEF estimated by first-pass RVG (top) and by gated SPECT (bottom). FP = first-pass; LVEF = left ventricular ejection fraction; and RVG = radionuclide ventriculography.

Comparison of Quantitative Sestamibi Defect and Visual Analysis

Quantitative rest sestamibi defect size correlated closely with semiquantitative visual summed rest score of segments with score ≥2 and the numbers of abnormal segments (score ≥2) ($r = 0.82$ and $r = 0.77$, $n = 35$, Fig. 4). Similarly, quantitative defect severity correlated well with visual summed rest score and with the numbers of abnormal segments ($r = 0.86$ and $r = 0.76$, $n = 35$, Fig. 5).

DISCUSSION

Acute myocardial infarction results from decreased myocardial blood flow, which is readily visualized as a perfusion defect on myocardial perfusion imaging (*17*). In the chronic phase, myocardial infarction with subsequent fibrosis still demonstrates a resting perfusion defect because of loss of myocardial mass and the lower tissue blood flow to fibrotic myocardium. Global contractile performance as assessed by ejection fraction declines acutely in direct relation to the extent of the histological damage (*18*) and in the absence of reperfusion remains

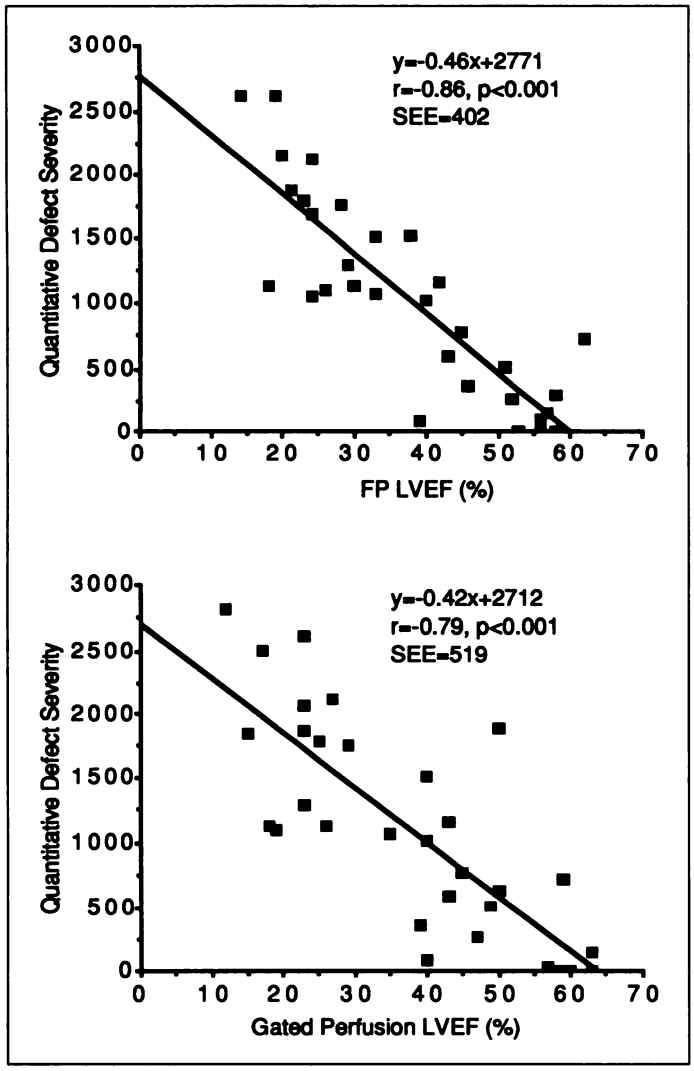

FIGURE 3. Correlation between quantitative rest ^{99m}Tc-sestamibi perfusion defect severity and LVEF estimated by first-pass RVG (top) and by gated SPECT (bottom). FP = first-pass; LVEF = left ventricular ejection fraction; and RVG = radionuclide ventriculography.

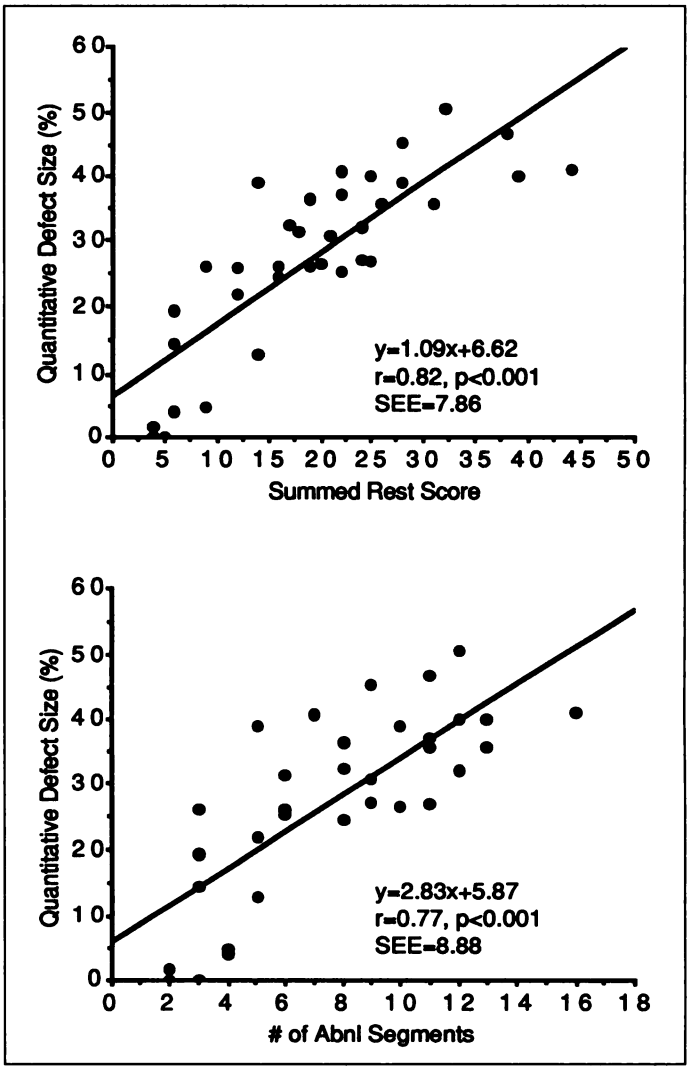

FIGURE 4. Correlation between quantitative rest ^{99m}Tc-sestamibi perfusion defect size and visual summed rest score of abnormal segments (top) and the number of abnormal segments (bottom).

depressed over time (*19*). In other animal studies, Pfeffer and Braunwald found an r value of −0.79 between EF and histologically determined myocardial infarct size in rats with healed (>2 wk) myocardial infarction (*20*). The results of the present study in patients with remote prior myocardial infarction indicate that quantitation of rest sestamibi SPECT defect extent and severity by using the automatic CEqual program correlates well with rest LVEF and with semiquantitative expert visual defect analysis. These findings, in conjunction with prior experimental data (*1–4*), suggest that quantitative rest ^{99m}Tc-sestamibi can accurately measure infarct size.

Technetium-99m-sestamibi perfusion imaging has been shown previously to be valuable for assessing myocardium at risk and final infarct size using tomographic imaging, and to correlate closely with ejection fraction measurements (*21,22*). Using a different quantitative technique, Christian et al. (*2*) demonstrated a close correlation between perfusion defect size and ejection fraction at discharge (r = −0.87), 6 wk (r = −0.81) and 1 yr (r = −0.78) after MI. Similar but somewhat lower correlation with an r value of −0.63 between total perfusion defect size and LVEF during transient coronary occlusion was observed in a study by Gallik et al. (*23*). However, in patients undergoing reperfusion therapy, the ejection fraction at discharge can be significantly lower than that predicted on the basis of perfusion defect size (*22,24*), principally due to stunned myocardium. Conversely, due to early compensatory hyperkinesis and subsequent late remodeling, ejection fraction at discharge maybe higher than at 6 wk (*22*). In fact, a study by Chareonthaitawee et al. (*25*) from the same laboratory noting excellent correlation between perfusion defect size and ejection fractions at discharge (*2*) demonstrated that the correlation of rest perfusion defect size to ejection fraction rose from r = −0.39 at discharge to r = −0.84 at 1 yr. In the second article, Chareonthaitawee et al. (*25*) also noted that ejection fraction tended to be lower at the delayed measurement with the fall attributed to ventricular remodeling. The degree of LV remodeling after myocardial infarction is linearly related to infarct size. The major discrepancy in the ejection fraction correlations at the time of discharge and the perfusion defect size in these two articles were explained by the use of different methods (*25*). In the present study, to avoid the potential effect of myocardial stunning early after acute myocardial infarction as well as the problem of compensatory hyperkinesis, all patients were studied at least 30 days following myocardial infarction.

This study used automatic quantitative analysis of perfusion defect magnitude. Based on optimized acquisition, processing and quantitative protocols for ^{99m}Tc-sestamibi myocardial perfusion SPECT, Van Train et al. (*13*) previously developed

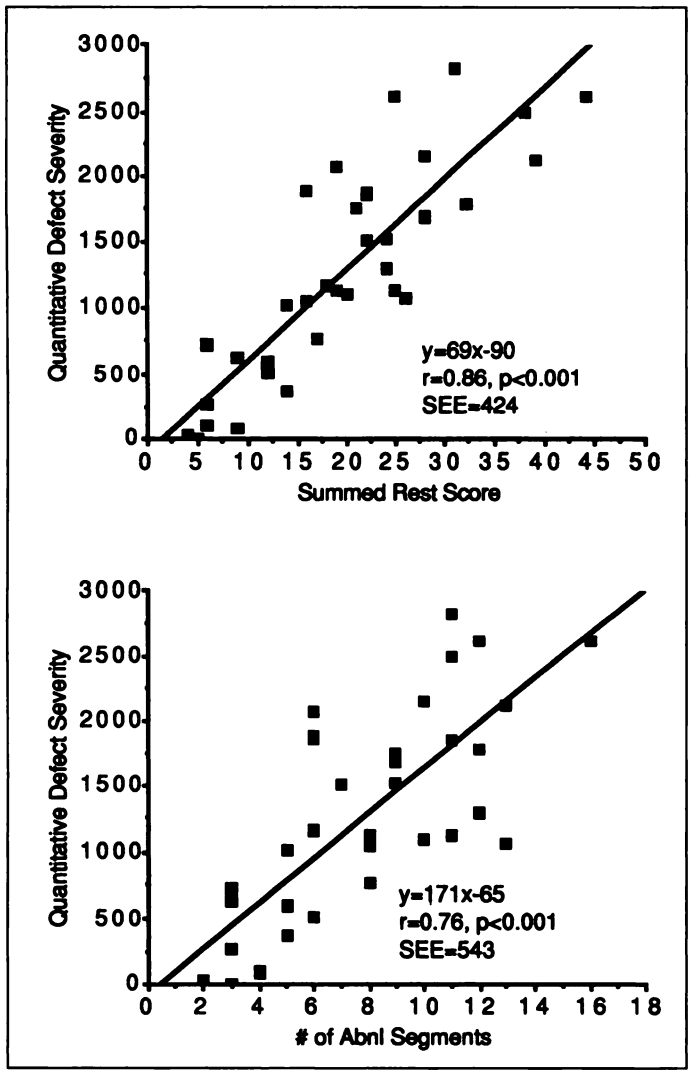

FIGURE 5. Correlation between quantitative rest ^{99m}Tc-sestamibi perfusion defect severity and visual summed rest score of abnormal segments (top) and the number of abnormal segments (bottom).

normal limits and criteria for abnormality for quantitative analysis of rest and stress ^{99m}Tc-sestamibi SPECT. The present study used the further development of high-dose ^{99m}Tc-sestamibi normal limits and an automatic quantitative program to measure perfusion defect extent and severity. The automatic program avoids potential problems of intra- and interobserver variability, which may arise from semi-automatic operation (*26*). We have previously demonstrated that even this semi-automatic quantitative analysis is highly reproducible when performed with exercise studies, a protocol that adds greater challenge to repeated measurements than the serial resting studies, showing r = 0.97 for global extent and r = 0.99 for global severity (*27*).

Previous studies have demonstrated that quantitative defect extent in exercise ^{99m}Tc-sestamibi myocardial perfusion has a high degree of accuracy for detection and localization of coronary artery disease (*28*) and correlates well with expert visual analysis (*13,28*). Using ^{201}Tl, we have also demonstrated that quantitative defect severity predicted the severity of the underlying coronary stenoses on coronary angiography (*29*). The current study showed that both quantitative defect extent and severity by rest sestamibi SPECT correlated closely with expert visual interpretation of the summed rest score and the number of abnormal segments. Higher correlations for quantitative defect severity were found with the summed rest score than with the number of abnormal segments. This is not surprising because quantitative defect severity and the summed rest score take into account both defect extent and defect severity, whereas the number of abnormal segments reflects only defect extent. Similarly, the highest correlations with LVEF and perfusion measurements were found with quantitative defect severity. This is also not unexpected since LVEF is affected by both extent and severity of contractile impairment.

The correlation between quantitative rest sestamibi defect size and LVEF tended to be higher in patients with anterior wall defects than in those with inferior wall defects. Inferior myocardial infarctions have been shown to generally have less hypoperfused myocardium than anterior infarctions (*21*), and the inferior wall of the LV of both men and women normally exhibits a greater variation in the normal range of apparent uptake due to the variable attenuation artifact. Further assessment of the regional variations and the potential gender differences should be accomplished by validation in greater numbers of patients. As a group, the patients in this study had relative low ejection fractions. The reason is related to the clinical indications for resting sestamibi studies which are often performed as a part of myocardial viability assessment in patients with large perfusion defects on stress sestamibi imaging or extensive functional abnormalities by contrast ventriculography or echocardiography.

First-pass radionuclide ventriculography is well established for the noninvasive assessment of cardiac performance. Close correlation (r = 0.84) has been shown for LVEF in comparison between FP RVG and contrast left ventriculography (*30*). Agreement between LVEF measured from rest-gated SPECT and FP RVG was high in a previous study from our group (r = 0.91, (*11*)) and in the present study (r = 0.96).

Study Limitations

The present study was performed in a relatively small group. Assessments of regional function in an attempt to estimate infarct size were not performed in this study since validated objective measurements of regional function are not available. Although global LV function is clinically more important, it is affected by the compensatory hyperkinesis of myocardial regions not involved by infarction. This limitation may well be responsible for the correlation between perfusion defect size and ejection fraction being high, in our and other studies, as opposed to very high. There was no attempt to compensate for image attenuation correction or scatter. Failure to make these corrections in women with large breasts or obese patients can result in artifactual perfusion defects, a cause of mismatch between defect size and LV function, and also has the effect of widening the normal limit for quantitative perfusion defect assessment. Furthermore, direct clinical quantitation of infarct size was not possible in this study. To confirm the accuracy of the quantitative program, experimental animal or autopsy studies may be important. The study employed a modification of the commercially available CEqual program which makes it automatic. The results of this modified program correlate well with those of the standard program when run by an experienced computer operator (*26*), providing the appropriate high dose resting normal limits are employed.

CONCLUSION

The results of this study define a strong relationship between measurements of ^{99m}Tc-sestamibi perfusion defect as measured by an automatic software program and global left ventricular function. The automatic quantitative program appears to be a useful measure of assessing infarct size in patients with remote myocardial infarction.

REFERENCES

1. Verani MS, Jeroudi MO, Mahamarian JJ, et al. Quantification of myocardial infarction during coronary occlusion and myocardial salvage after reperfusion using cardiac imaging with technetium-99m-hexakis 2-methoxyisobutyl isonitrile. *J Am Coll Cardiol* 1988;12:1573–1581.
2. Christian TF, Behrenbeck T, Gersh BJ, Gibbons RJ. Relation of left ventricular volume and function over one year after acute myocardial infarction to infarct size determined by technetium-99m-sestamibi. *Am J Cardiol* 1991;68:21–26.
3. Medrano R, Lowry RW, Young JB, et al. Assessment of myocardial viability with ^{99m}Tc-sestamibi in patients undergoing cardiac transplantation. *Circulation* 1996;94: 1010–1017.
4. Miller TD, Christian TF, Hopfenspirger MR, Hodge DO, Gersh BJ, Gibbons RJ. Infarct size after acute myocardial infarction measured by quantitative tomographic ^{99m}Tc-sestamibi imaging predicts subsequent mortality. *Circulation* 1995;92:334–341.
5. Berman DS, Kiat H, Friedman JD, et al. Separate acquisition rest thallium-201/stress technetium-99m-sestamibi dual-isotope myocardial perfusion single-photon emission computed tomography: a clinical validation study. *J Am Coll Cardiol* 1993;22:1455–1464.
6. Feiring AJ, Johnson MR, Kioschos JM, Kirchner PT, Marcus ML, White CW. The importance of the determination of the myocardial area at risk in the evaluation of acute myocardial infarction in patients. *Circulation* 1987;75:980–987.
7. Schneider RM, Chu A, Akaishi M, Weintramb W, Morris K, Cobb F. Left ventricular ejection fraction after acute coronary artery occlusion in dogs: relationship to the extent and site of myocardial infarction. *Circulation* 1985;72:632–638.
8. Berman DS, Kiat H, Van Train K, Garcia E, Friedman JD, Maddahi J. Technetium-99m-sestamibi in the assessment of chronic coronary artery disease. *Semin Nucl Med* 1991;21:190–212.
9. Germano G, Kavanagh PB, Su H, et al. Automatic reorientation of three-dimensional, transaxial myocardial perfusion SPECT images. *J Nucl Med* 1995;36:1107–1114.
10. Germano G, Kavanagh PB, Chen J, et al. Operator-less processing of myocardial perfusion SPECT studies. *J Nucl Med* 1995;36:2127–2132.
11. Germano G, Kiat H, Kavanagh PB, et al. Automatic quantification of ejection fraction from gated myocardial perfusion SPECT. *J Nucl Med* 1995;36:2138–2147.
12. Garcia EV, Cooke D, Van Train KF, et al. Technical aspects of myocardial SPECT imaging with technetium-99m-sestamibi. *Am J Cardiol* 1990;66:23E–31E.
13. Van Train KF, Areeda J, Garcia EV, et al. Quantitative same-day rest-stress technetium-99m-sestamibi SPECT: definition and validation of stress normal limits and criteria for abnormality. *J Nucl Med* 1993;34:1494–1502.
14. Folks R, Garcia E, Van Train K, Areeda J, Berman D, DePuey E. Quantitative two-day ^{99m}Tc-sestamibi myocardial SPECT: multicenter trial validation of normal limits [Abstract]. *J Nucl Med Technol* 1996;24:158.
15. Benari B, Kiat H, Erel J, et al. Repeatability of treadmill exercise ejection fraction and wall motion using technetium-99m-labeled sestamibi first-pass radionuclide ventriculography. *J Nucl Cardiol* 1995;2:478–484.
16. Palmas W, Friedman JD, Diamond GA, Silber H, Kiat H, Berman DS. Incremental value of simultaneous assessment of myocardial function and perfusion with technetium-99m-sestamibi for prediction of extent of coronary artery disease. *J Am Coll Cardiol* 1995;25:1024–1031.
17. Wackers FJT, Sokole EB, Samson G, et al. Value and limitations of thallium-201 scintigraphy in the acute phase of myocardial infarction. *N Engl J Med* 1976;295:1–5.
18. Hori M, Inoue M, Mishima M, Shimazu T, Abe H, Fukui S. Infarct size and left ventricular ejection fraction in acute myocardial infarction. *Jpn Circ J* 1977;41:1299–1309.
19. Fletcher PJ, Pfeffer JM, Pfeffer MA, Braunwald E. Left ventricular diastolic pressure-volume relations in rats with healed myocardial infarction. *Circ Res* 1981;49:618–626.
20. Pfeffer MA, Braunwald E. Ventricular remodeling after myocardial infarction. *Circulation* 1990;81:1161–1172.
21. Gibbons RJ, Verani MS, Behrenbeck T, Pellikka PA, Mahmarian JJ. Feasibility of tomographic technetium-99m-hexakis-2-methoxy-2-methypropyl-isonitrile imaging for the assessment of myocardial area at risk and the effect of acute treatment in myocardial infarction. *Circulation* 1989;80:1277–1286.
22. Christian TF, Behrenbeck T, Pellikka PA, Huber KC, Chesebro JH, Gibbons RJ. Mismatch of left ventricular function and infarct size demonstrated by technetium-99m-isonitrile imaging after reperfusion therapy for acute myocardial infarction: Identification of myocardial stunning and hyperkinesia. *J Am Coll Cardiol* 1990;16: 1632–1638.
23. Gallik DM, Obermueller SD, Swarna US, Guidry GW, Mahmarian JJ, Verani MS. Simultaneous assessment of myocardial perfusion and left ventricular function during transient coronary occlusion. *J Am Coll Cardiol* 1995;25:1529–1538.
24. Leavitt JI, Getter N, Tow DE, Rocco TP. Demonstration of viable, stunned myocardium with technetium-99m-sestamibi. *J Nucl Med* 1994;35:1805–1807.
25. Chareonthaitawee P, Christian TF, Hirose K, Gibbons RJ, Rumberger JA. Relation of initial infarct size to extent of left ventricular remodeling in the year after acute myocardial infarction. *J Am Coll Cardiol* 1995;25:567–573.
26. Silagan G, Tecson J, Van Train K, et al. Manual versus automatic quantitative analysis of myocardial perfusion SPECT [Abstract]. *J Nucl Med Technol* 1996;24:173.
27. Kiat H, Bernari B, Williams C, et al. Reproducibility of quantitative rest thallium-201/stress ^{99m}Tc-sestamibi dual-isotope SPECT for assessment of perfusion defect extent and reversibility [Abstract]. *J Nucl Med* 1994;35(suppl):103P.
28. Van Train KF, Garcia EV, Maddahi J, et al. Multicenter trial validation for quantitative analysis of same-day rest-stress technetium-99m-sestamibi myocardial tomograms. *J Nucl Med* 1994;35:609–618.
29. Matzer L, Kiat H, Van Train K, et al. Quantitative severity of stress thallium-201 myocardial perfusion single-photon emission computed tomography defects in one-vessel coronary artery disease. *Am J Cardiol* 1993;72:273–279.
30. Takeishi Y, Sukekawa H, Saito H, et al. Left ventricular function and myocardial perfusion during dipyridamole infusion assessed by a single injection of ^{99m}Tc-sestamibi in patients unable to exercise. *Nucl Med Commun* 1994;15:697–703.